

1 **A Multi-Scale Daily SPEI Dataset for Drought characterizing at Observation**

2 **Stations over the Mainland China from 1961 to 2018**

3 Qianfeng Wang^{a, c*}, Jingyu Zeng^a, Junyu Qi^b, Xuesong Zhang^{b, c}, Yue Zeng^a, Wei Shui^a,

4 Zhanghua Xu^a, Rongrong Zhang^a, Xiaoping Wu^a

5 a. Fujian Provincial Key Laboratory of Remote Sensing of Soil Erosion and Disaster

6 Protection/College of Environment and Resource, Fuzhou University, Fuzhou,

7 350116, China

8 b. Earth System Science Interdisciplinary Center, University of Maryland, College

9 Park, 5825 University Research Ct, College Park, MD, 20740, USA

10 c. Joint Global Change Research Institute, Pacific Northwest National Laboratory

11 and University of Maryland, College Park, MD 20740, USA

12

13

14

15

16

17

18

19

20

21

*Corresponding author: Qianfeng Wang

E-mail:wangqianfeng@fzu.edu.cn

22 **Highlights:**

- 23 • A multi-scale daily SPEI dataset was developed across the mainland China from
24 1961 to 2018.
- 25 • The daily SPEI dataset can be used to identify the start and end day of the drought
26 event.
- 27 • The developed daily SPEI dataset in this study is free, open and persistent publicly
28 available.

29

30

31

32

33

34

35

36

37

38

39

40

41

42

43

44

45 **Abstract:**

46 The monthly Standardized Precipitation Evapotranspiration Index (SPEI) can be used
47 to monitor and assess drought characteristics with one month or longer drought
48 duration. Based on data from 1961 to 2018 at 427 meteorological stations across the
49 mainland China, we developed a daily SPEI dataset to overcome the shortcoming of
50 coarse temporal scale of monthly SPEI. Our dataset not only can be used to identify
51 the start and end dates of drought events, but also can be used to investigate the
52 meteorological, agricultural, hydrological and socioeconomic droughts with different
53 time scales. In the present study, the SPEI data with 3-month (about 90 days) scale
54 were taken as a demonstration example to analyze spatial distribution and temporal
55 changes in drought conditions for the mainland China. The SPEI data with 3-month
56 (about 90 days) scale showed no obvious intensifying trends in terms of severity,
57 duration, and frequency of drought events from 1961 to 2018. Our drought dataset
58 serves as a unique resource with daily resolution to a variety of research communities
59 including meteorology, geography, and natural hazard studies. The daily SPEI dataset
60 developed is free, open and persistent publicly available from this study. The dataset
61 with daily SPEI is publicly available via the figshare portal (Wang et al, 2020c), with
62 <https://doi.org/10.6084/m9.figshare.12568280>.

63 **Key words:**

64 **SPEI, mainland China, drought, spatial-temporal, Multi-scale, meteorological**
65 **data**

66

67

68 **1. Introduction**

69 Drought is one of the most destructive natural hazards worldwide. It can lead to
70 adverse effects to the ecological system, industrial production, agricultural practices,
71 drinking water availability, hydrological processes and water quality (Bussi and
72 Whitehead, 2020; Lai et al., 2019; Vicente-Serrano et al., 2012; Wang et al., 2014;
73 Wang et al., 2017). Drought has brought about ca. 221 billion dollars loss during 1960
74 to 2016 reported by the International Disaster Database (EM-DAT), and the drought
75 events in South Asia have influenced over 60 million residents from 1998 to 2001
76 (Agrawala et al., 2001). Unfortunately, the drought is expected to increase in
77 frequency and intensity due to the future warming air temperature (Trenberth et al.,
78 2014; Zambrano et al., 2018). The exacerbated drought conditions have promoted
79 some national legislation (such as drought preparedness and plan) to carry out the risk
80 management and adaptive strategy for drought disasters (Garrick et al., 2017).

81 The various drought types result in the difficulty of drought characterizing and
82 assessment. Drought definition is not unique. Some proposed defining drought
83 according to the water deficit (Wilhite and Glantz, 1985), while others defined
84 drought based on the period of abnormal arid conditions (Eslamian et al., 2017). The
85 popular drought can be classified into four types including (1) meteorological, (2)
86 agricultural, (3) hydrological, and (4) socioeconomic droughts (Mishra and Singh,

87 2010). The meteorological drought results from precipitation deficit or evaporation
88 increases (McKee et al., 1993). The meteorological drought can propagate into the
89 agricultural drought with the lower soil moisture availability, and it also can lead to
90 hydrological drought with lower streamflow and socioeconomic drought with lower
91 water availability (Barella-Ortiz and Quintana-Seguí, 2019; Gevaert et al., 2018). In
92 general, drought indices are normally used to monitor and assess the condition or
93 spatial-temporal characteristic of drought.

94 Many drought indices have been developed for the drought characterizing and
95 assessment, such as the Palmer drought severity index (PDSI) (Dai et al., 2004),
96 standardized precipitation index (SPI) (McKee et al., 1993), vegetation water supply
97 index (VWSI) (Carlson et al., 1994), vegetation health index (VHI) (Kogan, 2002),
98 vegetation temperature condition index (VTCI) (Wan et al., 2004), and other drought
99 indices (Men-xin and Hou-quan, 2016; Wang et al., 2015; Wang et al., 2017). PDSI
100 and SPI are the most popular drought studies worldwide (Dai et al., 2004; McKee et
101 al., 1993), however, they have some limitations. PDSI is only suitable to the
102 agricultural drought through characterizing the soil water deficit, and it cannot
103 identify the meteorological, hydrological, and socioeconomic droughts (Feng and Su,
104 2019). In addition, PDSI limits the spatial comparability of drought due to the fact
105 that it is heavily depending on data calibration (Sheffield et al., 2009; Yu et al., 2014).
106 Although the SPI can be used to monitor and assess different drought types by
107 multiple spatial scales at the monthly time step, it only considers the precipitation
108 factor and neglects effects of evaporation stemmed from temperature and other

109 meteorological factors (Wang et al., 2014; Wang et al., 2017; Yang et al., 2018). To
110 solve the above problems, the Standardized Precipitation Evapotranspiration Index
111 (SPEI), which considers the advantage of both PDSI and SPI, was developed to
112 monitor and assess droughts (Vicente-Serrano et al., 2010). It not only accounts for
113 the effect of evaporation on drought, but also have the capability of spatial
114 comparability and characterizing different drought types with multiple time scales
115 (Feng and Su, 2019; Wang et al., 2015). SPEI can be used to delineate
116 spatial-temporal evolution of drought, drought characteristics, and impacts of drought
117 at the regional and global scales (Mallya et al., 2016; Wang et al., 2014).

118 However, the commonly used SPEI fails to identify droughts with less than
119 one-month duration (Van der Schrier et al., 2011; Vicente-Serrano et al., 2010). With
120 the future climate change, flash droughts have been recently categorized as a type of
121 extreme climate events. Flash droughts occur along with sudden onset, rapid
122 aggravation, and sudden end of drought could lead to severe consequences
123 (Pendergrass et al., 2020). It is imperative for characterizing the flash droughts with
124 the short-term duration (e.g., several days). To use the sub-month resolution drought
125 index, we have developed the daily SPEI for the first time, and our daily SPEI has
126 been used to assess the drought and its impacts in previous studies (Wang et al., 2015;
127 Wang et al., 2017). The new SPEI can not only identify the drought with one-month
128 and more than one-month duration, but also monitor the drought with several days
129 duration. In addition, our new daily SPEI has filled the gap in the capability to
130 monitor the onset and duration of droughts. Our daily SPEI has similar principles with

131 the commonly used month SPEI in terms of time accumulation effects
132 (Vicente-Serrano et al., 2010; Wang et al., 2015; Yu et al., 2014). The daily SPEI data
133 with different time scales can also meet the requirement of characterizing and
134 assessing of different drought types (meteorological drought, agricultural drought and
135 hydrological drought) at multi-time scales (Wang et al., 2014).

136 The SPEI can be calculated by the difference between daily precipitation and
137 daily potential evapotranspiration (PET) (Vicente-Serrano et al., 2012). Precipitation
138 general can be directly obtained by the meteorological observation stations (Wang et
139 al., 2015). But PET can be only estimate by driver of meteorological data or remote
140 sensing data (Wang et al., 2018; Wang et al., 2017). Although there are at least 50
141 methods to calculate the PET potential evapotranspiration, the methods estimate the
142 inconsistent and different values due to diverse assumptions, data inputs and climatic
143 regions (Grismer et al., 2002; Lu et al., 2005). PET plays an important role in
144 understanding fluxes of the heat and mass of atmospheric system at the local and
145 global scale (Thomas, 2000). Thus, it is necessary to choose the suitable method to
146 estimate PET. The choice of candidate probability distributions for SPEI calculation is
147 also very important (Vicente-Serrano et al., 2010; Vicente-Serrano et al., 2012), the
148 chosen distribution for SPEI generally need a location parameter because climatic
149 water balance may have the negative values (when $PET >$ precipitation in certain a
150 periods) (Wang et al., 2015; Wang et al., 2017). Distributions for SPEI normalization
151 have generalized logistic distribution, Pearson Type III distribution, normal
152 distribution, generalized extreme value (GEV) distribution (Stagge et al., 2015). The

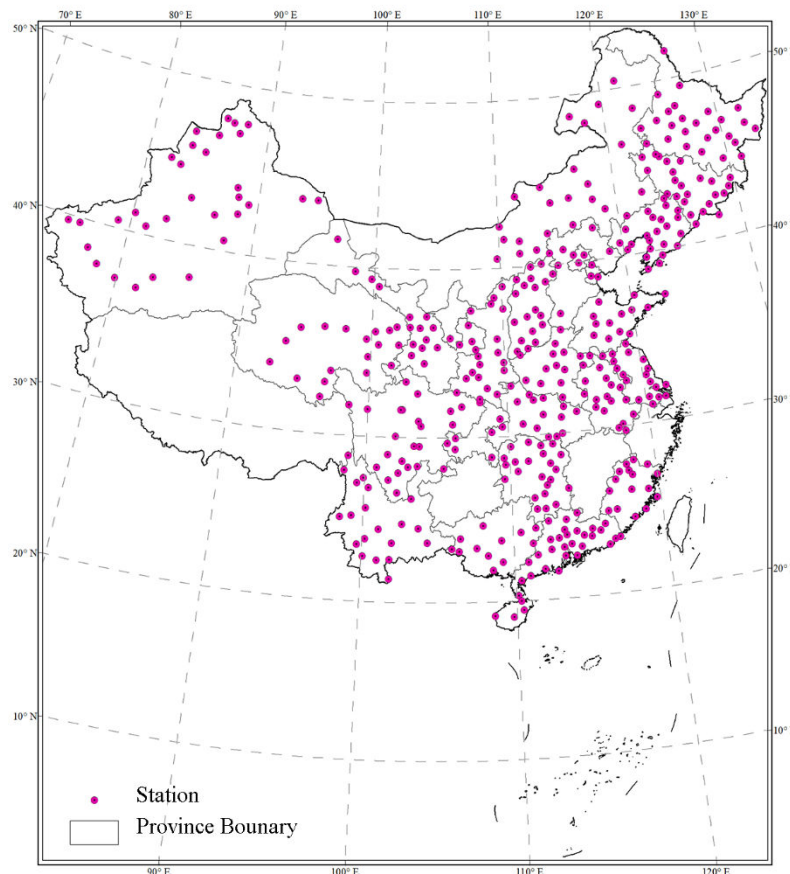
153 four candidate SPEI distributions have the best good-ness of fitting the accumulated
154 climatic water balance (Stagge et al., 2015; Wang et al., 2015; Wang et al., 2017).
155 However, The GEV distribution has the best performance among all four probability
156 distributions across the whole Continental Europe, because of the lower rejection
157 frequencies of GEV by using several tests (Kolmogorov–Smirnov (K–S), Anderson–
158 Darling (A–D), and Shapiro–Wilk (S–W)) (Stagge et al., 2015), therefore, we choose
159 the GEV distribution fitting he accumulated climatic water balance to calculate SPEI.
160 The SPEI are suited to investigate the effect of climate change and global warming on
161 drought severity. SPEI has been widely used in diverse studies on drought variability
162 and impact, and drought monitoring systems (Boroneant et al., 2011; Fuchs et al.,
163 2012; Potop et al., 2014; Sohn et al., 2013).

164 The aim of this study, therefore, is to produce a long record (1961-2018) daily
165 drought index dataset for the whole mainland China. Specifically, we used the new
166 daily SPEI algorithm to produce the multi-time scale drought dataset at a daily time
167 resolution. Meteorological data with 427 stations including multi-factor (daily
168 precipitation, daily average air temperature, daily minimum air temperature, daily
169 maximum air temperature and sunshine) are used. The developed drought dataset at
170 the national scale has the potential to be used to monitor and assess droughts and their
171 impacts for the sectors including agricultural sector, forest sector, hydrological sector,
172 ecological sector, environmental sector and so on.

173 **2. Data Sources and Methods**

174 **2.1 Data Sources**

175 Daily meteorological data from 1960 to 2018 were collected from the National
176 Meteorological Science Data Sharing Service Platform (<http://data.cma.cn/>). The data,
177 which have gone through quality controlling, have been used in many studies on
178 drought (Li et al., 2019; Wang et al., 2019). In total, there are 839 stations with public
179 data. To ensure continuous and complete data records, 427 meteorological stations are
180 chose for our study by removing stations with missing data exceeding 30 days over
181 the whole period. Meteorological variables include the minimum and maximum air
182 temperature (°C), precipitation (mm) and sunshine duration (h). The sunshine duration
183 was converted to solar radiation based on the Ångström function (Chen et al., 2010;
184 Wang et al., 2015). The station location is shown in Figure 1.



185

186 **Figure 1.** The location of meteorological stations across the mainland China.

187 2.2 Daily SPEI Calculation

188 The daily SPEI can be calculated by the difference between daily precipitation
189 and daily potential evapotranspiration. Because air temperature and solar radiation
190 explained at least 80% of evapotranspiration variability (Martí et al., 2015; Priestley
191 and Taylor, 1972), the Hargreaves model based on temperature and solar radiation can
192 be used to estimate the daily potential evapotranspiration (Hargreaves and Samani,
193 1982; Mendicino and Senatore, 2013; Wang et al., 2015). The daily potential
194 evapotranspiration can be obtained by the following formula:

$$195 \quad PET = 0.0023 * (T_{mean} + 17.8) * \sqrt{(T_{max} - T_{min})} * R_a \quad (1)$$

196 where, T_{mean} is the daily average air temperature ($^{\circ}\text{C}$); T_{max} and T_{min} are the daily
197 maximum and minimum air temperatures ($^{\circ}\text{C}$), respectively; and R_a is the daily net
198 radiation on the land surface ($\text{MJ m}^{-2} \text{d}^{-1}$).

199 SPEI calculation depends on the accumulating deficit or surplus (D_i) of water
200 balance at different time scales. D_i can be determined based on precipitations (P) and
201 PET formula given day i :

$$202 \quad D_i = P_i - PET_i \quad (2)$$

203 The obtained D_i values are summed at different time scales, following the same
204 procedure as that for the commonly used SPEI. The $D_{i,j}^k$ in a given day j and year
205 i depends on the chosen time scale k (days). For example, the accumulated difference
206 for 1 day in a particular year i with a 30-day (or other time scales) time scale is

207 calculated using:

$$\begin{aligned}
 X_{i,j}^k &= \sum_{l=31-k+j}^{30} D_{i-1,l} + \sum_{l=1}^j D_{i,l} , & \text{if } j < k \text{ and} \\
 X_{i,j}^k &= \sum_{l=j-k+1}^j D_{i,l} , & \text{if } j \geq k
 \end{aligned}
 \tag{3}$$

209 We also need to normalize the water balance into a probability distribution to get
 210 the SPEI index series. The best distribution for SPEI calculation is the generalized
 211 extreme value (GEV) distribution (Stagge et al., 2015), which can overcome the
 212 limitation of original SPEI through generalized logistic distribution for short
 213 accumulation (1–2 months) periods (Stagge et al., 2015; Vicente-Serrano et al., 2010).
 214 Therefore, we adopted the GEV distribution to standardize the D series into SPEI data
 215 series (Monish and Rehana, 2020). The GEV probability density function is:

$$f(x) = \begin{cases} \left(\frac{1}{\sigma}\right) \left[(1 + \xi z(x))^{-1/\xi} \right]^{\xi+1} e^{-[(1+\xi z(x))^{-1/\xi}]}, & \xi \neq 0, \quad 1 + \xi z(x) > 0 \\ \left(\frac{1}{\sigma}\right) e^{-z(x) - e^{-z(x)}}, & \xi = 0, \quad -\infty < x < \infty \end{cases}
 \tag{4}$$

217 where,

$$z(x) = \frac{x - \mu}{\sigma}
 \tag{5}$$

218 where, ξ , σ , and μ are the shape, scale, and location parameters respectively. The
 219 cumulative distribution function $F(x)$ of GEV can be calculated by the following
 220 equation:
 221

$$F(x) = e^{-t(x)}
 \tag{6}$$

222 where,

$$t(x) = \begin{cases} \left(1 + \xi \left(\frac{(x - \mu)}{\sigma}\right)\right)^{-\frac{1}{\xi}}, & \text{if } \xi \neq 0 \\ e^{-(x - \mu)/\sigma}, & \text{if } \xi = 0 \end{cases} \quad (7)$$

Thus, the probability distribution function of the D series is given by:

$$F(x) = \left[1 + \left(\frac{\alpha}{x - \gamma}\right)^\beta\right]^{-1} \quad (8)$$

With $F(x)$, the SPEI can easily be obtained as the standardized values of $F(x)$.

Following the classical approximation of Abramowitz and Stegun (1965):

$$SPEI = W - \frac{C_0 + C_1W + C_2W^2}{1 + d_1W + d_2W^2 + d_3W^3} \quad (9)$$

where, $W = \sqrt{-2 \ln(P)}$ for $P \leq 0.5$ and P is the probability of exceeding a determined D value, $P = 1 - F(x)$. If $P > 0.5$, then P is replaced by $1 - P$ and the sign of the resultant SPEI is reversed. The constants are $C_0 = 2.515517$, $C_1 = 0.802853$, $C_2 = 0.010328$, $d_1 = 1.432788$, $d_2 = 0.189269$, and $d_3 = 0.001308$.

2.3 Drought Analysis Method

The daily SPEI dataset were calculated in five accumulating periods (30 days, 90 days, 180 days months, 360 days, 720 days) based on the water balance (difference between precipitation and PET). The classifications for the SPEI drought classes are presented in Table 1.

241

Table 1 Categorization of drought and wet grade according to the SPEI(Wang et al., 2014).

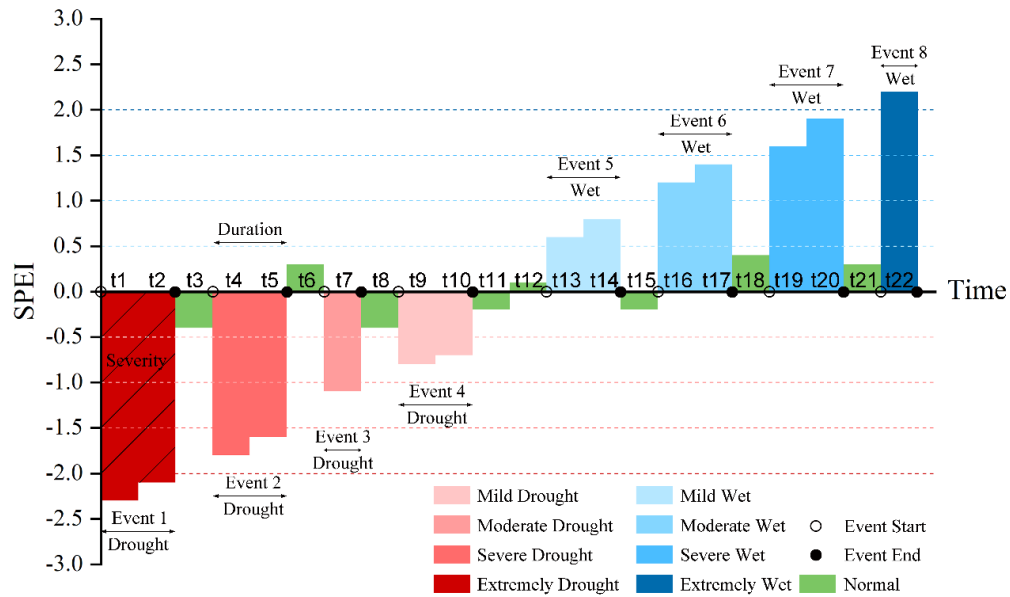
| Categorization | SPEI values |
|----------------|---------------------|
| Extremely Wet | $SPEI \geq 2$ |
| Severe Wet | $1.5 \leq SPEI < 2$ |
| Moderate Wet | $1 \leq SPEI < 1.5$ |

| | |
|-------------------|----------------------------------|
| Mild Wet | $0.5 < \text{SPEI} < 1$ |
| Normal | $-0.5 \leq \text{SPEI} \leq 0.5$ |
| Mild Drought | $-1 < \text{SPEI} < -0.5$ |
| Moderate Drought | $-1.5 < \text{SPEI} \leq -1$ |
| Severe Drought | $-2 < \text{SPEI} \leq -1.5$ |
| Extremely Drought | $\text{SPEI} \leq -2$ |

244

245 We used the method described by Yevjevich (1967) to define the drought
246 characteristics (severity, duration, and intensity). A drought event can be firstly
247 determined by drought start and end dates, and its duration and severity were then
248 assigned. Thus, we accounted for the continuity of drought propagation. The
249 continuous days with SPEI values less than the threshold (such as -0.5,-1.0,-1.5,-2)
250 are defined as the duration of a drought event. The severity is the integral area
251 between absolute value of the SPEI with value < -0.5 and the horizontal axis ($\text{SPEI} = 0$)
252 from the drought start day to the drought end day. The drought frequency is the total
253 number of drought events in a period. The drought event and its characteristics
254 (severity, duration, and intensity) can be demonstrated in Figure 2.

255



256

257 **Figure 2.** Schematic diagram of drought and wet events (the red shaded area
 258 denotes the drought events; the blue shaded area denotes the wet events).

259

260 The SPEI data based on 90-day (3-month) time scales can be used to identify soil
 261 moisture or agriculture droughts (Wang et al., 2014). Due to its important applications,
 262 we selected the SPEI data with the 90-day time scales as the example data for
 263 analyzing in the present study. To investigate the spatial-temporal characteristics of
 264 the example data, we defined three variables including Annual Total Drought Severity
 265 (ATDS), Annual Total Drought Duration (ATDD), and Annual Total Drought
 266 Frequency (ATDF). The three variables were obtained by summing the severity,
 267 duration, and frequency of all the drought events in each year at 427 stations.

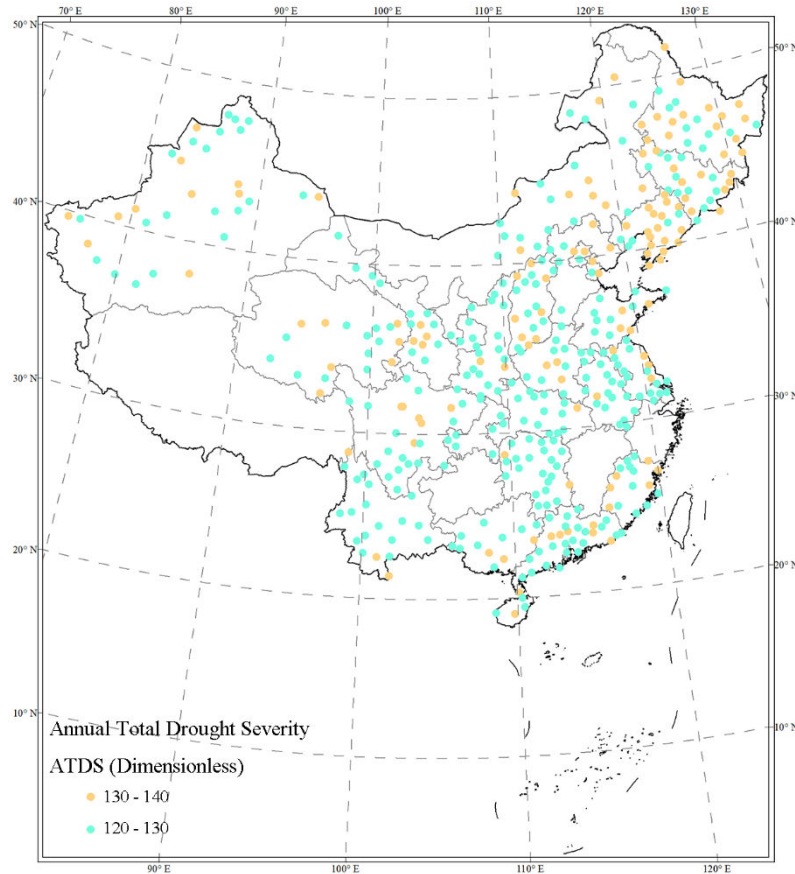
268 We also used the non-parametric Mann–Kendall (MK) test to detect monotonic
 269 trends (Kendall, 1948; Mann, 1945), because MK test does not require data normality
 270 (Mann, 1945; Wang et al., 2020a; Wang et al., 2020b). We computed slopes for ATDS,
 271 ATDD and ADF using the Sen’s method (Sen, 1968). These statistical methods are

272 commonly used in analyses of water resources, climate, and ecology data. For the MK
273 test, the global trend for the entire series is significant when $P\text{-value} < 0.05$.

274 **3 Analysis Results**

275 **3.1 Spatial Distribution of Drought Characteristics**

276 The ATDS can be used to identify hot spots with more severe drought conditions.
277 Figure 3 shows the calculated ATDS values across the mainland China. We
278 categorized ATDS values into two main groups with higher ATDS values indicated
279 more severe drought conditions. The distribution of ATDS values shows that, in
280 general, northeastern parts of China had more severe drought conditions than southern
281 parts. However, our results also indicate that the humid climate zone in the south also
282 experienced severe drought conditions, though not as much as for northern parts of
283 China (Figure 3).



284

285

Figure 3. The spatial distribution of ATDS across the mainland China.

286

287

Figure 4 shows that ATDD values ranged from 100 to 110 days for most stations

288

across the mainland China. This indicates that there was near one-third of a year when

289

most stations were experiencing drought conditions. More stations with ATDD values

290

ranging from 100 to 110 were found compared with stations with ATDD values of

291

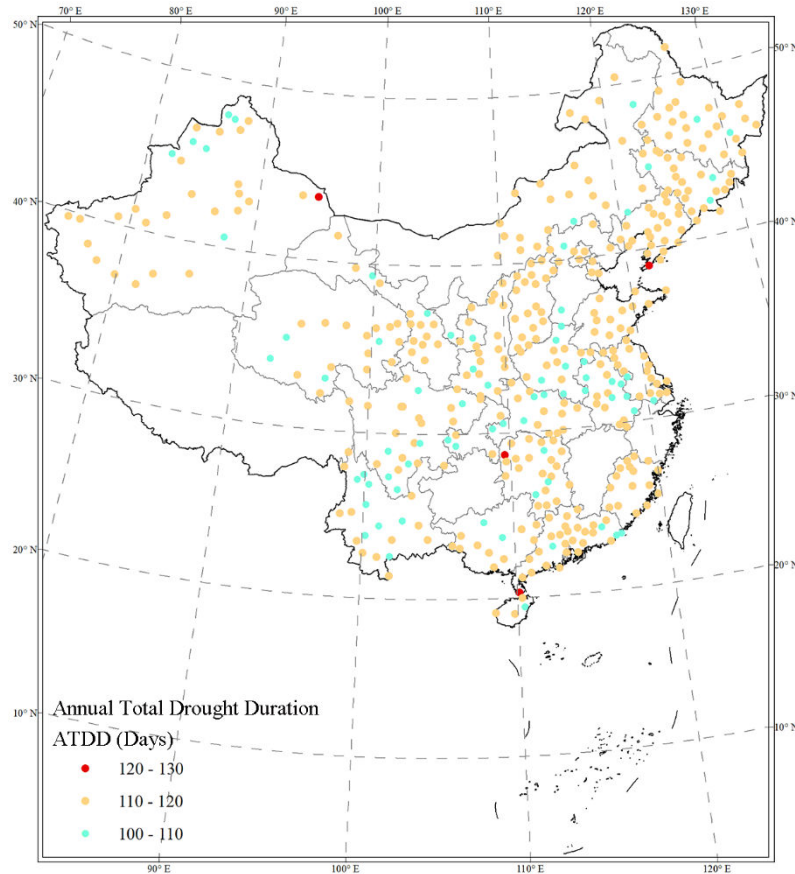
120-130 (Fig. 4). For drought years, the duration days of drought events are expected

292

to be were longer. The ATDD had similar spatial distribution characteristics with the

293

ATDS, indicating that droughts also occurred in the humid climate zone.



294

295

Figure 4. The spatial distribution of ATDD across the mainland China.

296

297 Figure 5 shows the spatial distribution of ATDF values across the mainland China.

298 In general, most stations had 4-6 annual drought events. There were fewer stations

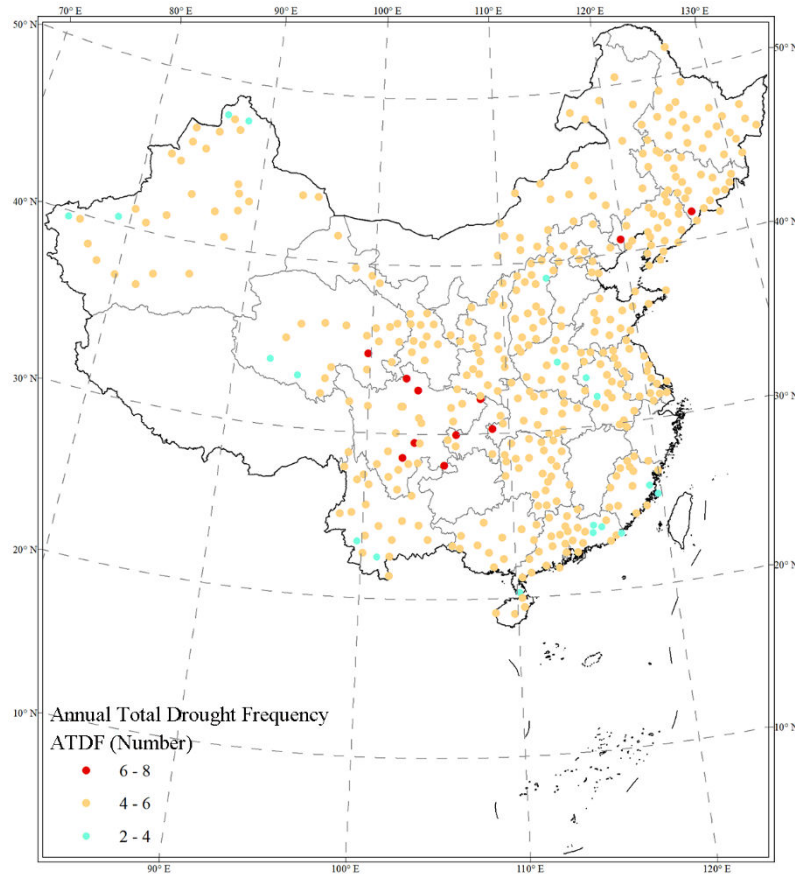
299 with 6-8 annual drought events compared with stations with 2-4 annual drought

300 events. We also detected that drought events could be occurring in both arid and

301 humid regions based on spatial distributions of ATDF values (Figure 5). Since the

302 ATDF indicated only the annual average drought events, we could expect that for the

303 severer drought years the ATDF would have greater values for different stations.

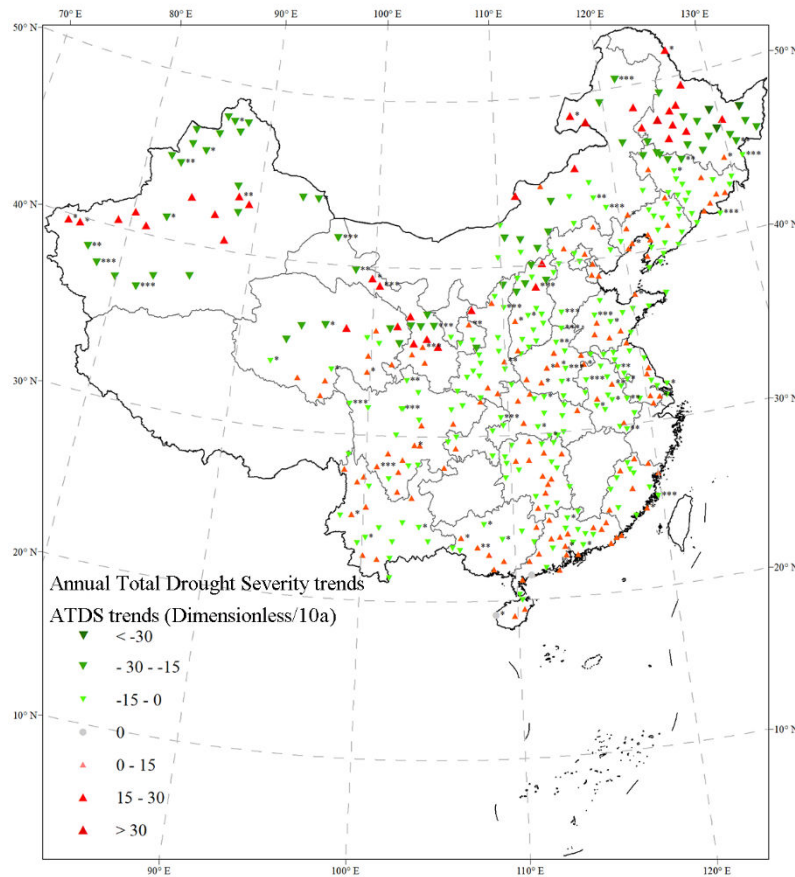


304
 305 **Figure 5.** The spatial distribution of ATDF across the mainland China.

306
 307 **3.2 Trends in Drought Characteristics**

308 The changing trends of ATDS can be used to detect whether drought severity is
 309 weakening or intensifying with time, Figure 6 shows that the spatial distribution of
 310 changing trends of ATDS from 1961 to 2018 across the mainland China. In general,
 311 there were more stations with weakening trends in drought severity than those with
 312 intensifying trends across all stations (Figure 6). It seems that both weakening and
 313 intensifying absolute values were largest in the northeast, northwest, and central
 314 China compared with other parts. However, after scrutiny, we found that drought
 315 severity tended to weaken in the northeast, northwest, and center China with more

316 stations having significant weakening trends by statistical test ($P\text{-value} < 0.05$; Figure 6).
 317 For southern China, most stations had no significant trends in either weakening or
 318 intensifying of drought severity ($P\text{-value} > 0.05$; Figure 6).



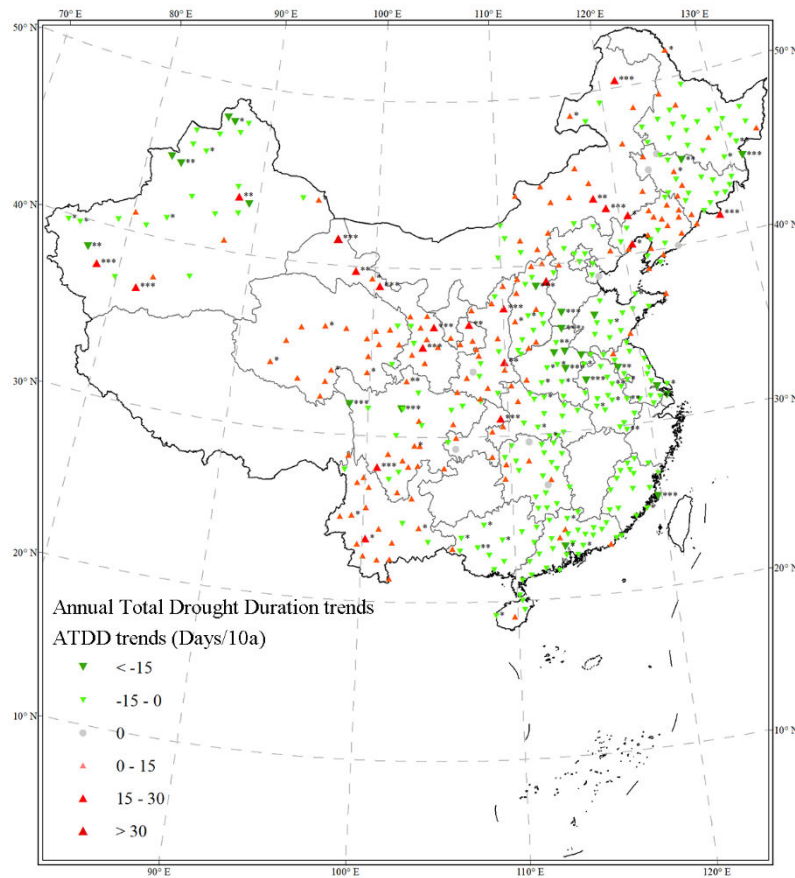
319
 320 **Figure 6.** The spatial distribution of the changing trends of ATDS (the red and green
 321 triangular indicate increasing and decreasing trends, respectively. “***” denotes
 322 $P\text{-value} < 0.001$, “**” denotes $P\text{-value} < 0.01$, and “*” denotes $P\text{-value} < 0.05$).

323

324 The changing trends of ATDD can be used to detect whether drought duration is
 325 getting shorter or longer. Figure 7 shows the spatial distribution of changing trends for
 326 the ATDD across all stations. In general, stations in the southeast demonstrated
 327 downward trends with shortening drought duration, while stations in the northwest

328 had upward trends for the ATDD with increasing drought duration (Figure 7). Note
329 that the increasing or decreasing trends for ATDD were significant (P value < 0.05)
330 for stations across the central China indicating that the central China regions were
331 suffering dramatic changes of drought conditions.

332



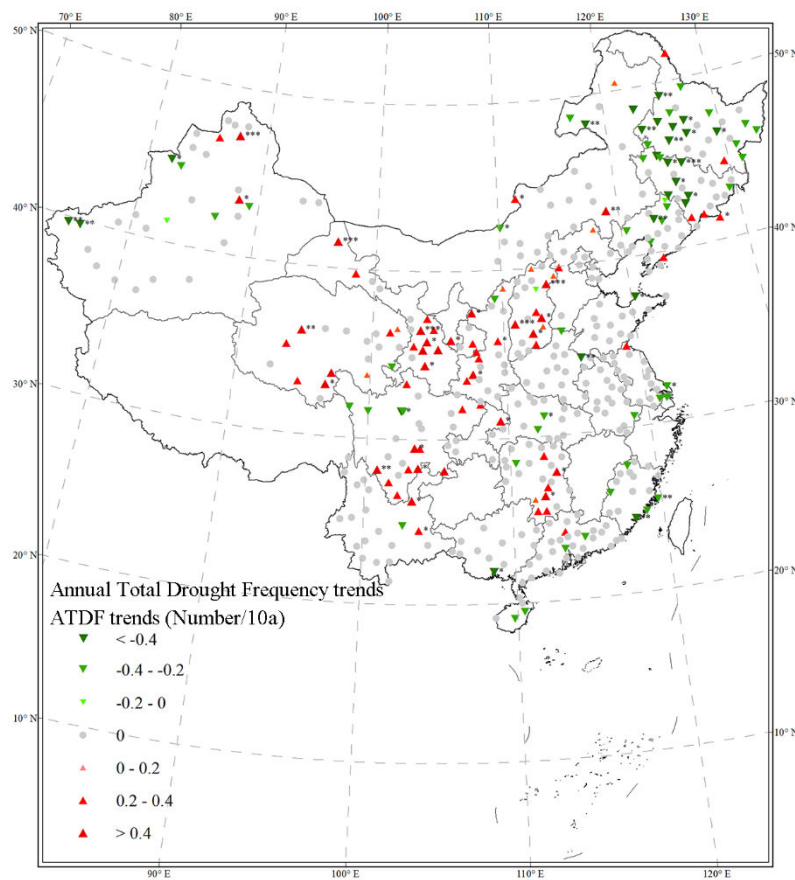
333

334 **Figure 7.** The spatial distribution of the changing trends of ATDD (the red and green
335 triangular indicate increasing and decreasing trends, respectively. “***” denotes
336 P-value < 0.001, “**” denotes P-value < 0.01, and “*” denotes P-value < 0.05).

337

338 The changing trends of ATDF can be used to detect whether the frequency of
339 drought events is increasing or decreasing with time. Figure 8 shows the spatial

340 distribution of changing trends of ATDF across all stations. Most stations
341 demonstrated no significant trend in the frequency of drought events, except for
342 dozens of stations in western China having significant upward trends (P-value < 0.05)
343 with increasing frequency in drought events, and stations in northeastern China
344 demonstrated significant downward trends (P-value < 0.05) with decreasing
345 frequency of drought events.



346
347 **Figure 8.** The spatial distribution of the changing trends of ATDF (the red and green
348 triangular indicate increasing and decreasing trends, respectively. “***” denotes
349 P-value < 0.001, “**” denotes P-value < 0.01, and “*” denotes P-value < 0.05).

350

351

352 **4. Discussion**

353 The reason for selecting 90 days (3-month) scale to assess spatial and temporal
354 characteristics of drought conditions across the mainland China is because the SPEI
355 with the 90 days (3-month) scale can indicate the agricultural drought (or soil
356 moisture) (Van der Schrier et al., 2011; Wang et al., 2014; Wang et al., 2017), and its
357 results are comparable with the PDSI (Dai et al., 2004; Van der Schrier et al., 2011)
358 and other drought indices including Surface Water Supply Index (SWSI) and Moisture
359 Adequacy Index (MAI) (Doesken and Garen, 1991; McGUIRE and Palmer, 1957).
360 The commonly used monthly SPEI have been used to assess drought characteristics
361 and their impacts worldwide from the regional scale to the global scale (Stagge et al.,
362 2015; Vicente-Serrano et al., 2010; Wang et al., 2014). The SPEI with different time
363 scales is relevant for meteorological drought (1-month timescale), agricultural drought
364 (3-6-month timescale about 90-180 days), hydrological drought (12-month timescale
365 about 360 days), and socioeconomic drought (24-month timescale about 720 days),
366 respectively (Homdee et al., 2016; Potop et al., 2014; Tirivarombo et al., 2018;
367 Vicente-Serrano et al., 2010).

368 Our new SPEI dataset with multi-time scales were developed and compiled using
369 the daily SPEI algorithm in the previous study (Wang et al., 2015). The daily SPEI
370 has been used in drought characterizing and assessment, and was validated by drought
371 characterizing and assessment (Jevšenak, 2019; Jia et al., 2018; Salvador et al., 2019;
372 Wang et al., 2015; Wang et al., 2017). The global SPEI database with monthly

373 temporal resolution and 0.5 degree spatial resolution is available
374 (<https://spei.csic.es/database.html>). The database covers the period between January 1901
375 and December 2018. Although the database can be used effectively for the
376 meteorological, agricultural, hydrological, and socioeconomic droughts, it cannot
377 identify and detect the flash drought with less than one-month duration. In addition,
378 the monthly database can only detect the start month and end month of drought events,
379 and therefore it fails to determine the start and end dates of a drought event, (Kassaye
380 et al., 2020; Vicente-Serrano et al., 2010; Wang et al., 2014). Our newly developed
381 daily SPEI can compensate the shortcomings of monthly SPEI in drought
382 characterizing and assessment. In addition, we used the well-received GEV
383 probability distribution for the SPEI calculation for our dataset (Stagge et al., 2015).

384 Although the daily SPEI has better performance in drought characterizing and
385 assessment (Jevšenak, 2019; Wang et al., 2017), the uncertainty of daily SPEI still
386 needs to be evaluated in future works. Our daily SPEI dataset used the simple
387 Hargreaves model based on temperature and solar radiation to estimate daily potential
388 evapotranspiration (Hargreaves and Samani, 1982; Wang et al., 2017). We will further
389 investigate effects of various evapotranspiration models (such as CRAE model,
390 Penman algorithm, Thornthwait algorithm, Makkink algorithm, and Priestley–Taylor
391 algorithm) on the calculation of SPEI (Makkink, 1957; Morton, 1983; Penman, 1948;
392 Priestley and Taylor, 1972; Thornthwaite, 1944). We only chose SPEI based on the
393 90 days (3-month timescale) as an example to analyze drought characteristics, and the
394 results demonstrated that there was no obvious intensifying trends for drought across

395 the mainland China which is consistent with other studies (Han et al., 2020).
396 Meanwhile, our newly developed daily SPEI will be further validated in other regions
397 of the world. In addition, SPEI values at different time scales can be used as a proxy
398 for other type of droughts but it lacks the complete picture (no soil moisture condition,
399 streamflow, etc.) (Zargar et al., 2011).

400 Our long-term daily SPEI dataset has contributed significantly to our
401 understanding of drought evolution, especially flash drought. The dataset can be used
402 to monitor and assess different drought types (meteorological drought, agricultural
403 drought, and hydrological drought) through different timescale data. It also can
404 identify the start and end dates for drought. The dataset is valuable to meteorological
405 research and natural hazards communities for various purposes such as assessment of
406 extreme climate or drought effect evaluation.

407 **5. Data Availability**

408 All daily SPEI dataset including data and their description at 427 observed
409 meteorological stations, the data is also provided as open access via figshare (Wang et
410 al, 2020c), available at doi.org/10.6084/m9.figshare.12568280. This depository includes
411 the five files directory of the daily SPEI data with five scales (30 days about 1 month,
412 90 days about 3 month, 180 days months about 6 month, 360 days about 12 month,
413 720 days about 24 month) and station information for 427 meteorological stations.

414

415

416 **6. Summary**

417 In the present study, we have produced a daily SPEI dataset from 1960 to 2018 at
418 427 meteorological stations across the mainland China. Our open-access dataset is an
419 important contribution to drought assessment, and it can overcome the disadvantages
420 of the commonly used monthly SPEI database. Our daily dataset can help monitor and
421 assess the spatial and temporal characteristics of droughts. It can be used to assess the
422 impacts of droughts on ecological system, hydrological processes, and other natural
423 resources. Our multi-time scale daily SPEI dataset can be widely used in studies on
424 meteorological drought (1-month timescale), agricultural drought (3-6-month
425 timescale), hydrological drought (360 days timescale), and socioeconomic drought
426 (24-month timescale). The dataset will reduce the time spent on research and avoid
427 the duplication of efforts, which will be highly attractive to meteorological,
428 geographical, natural hazard researchers and searchers from other areas.

429

430 **Author contributions.** QFW led the study, developed the method, and wrote the
431 manuscript with input from all the authors. JYQ and XSZ discussed the results and
432 revised the manuscript. All the authors contributed to the final manuscript. QFW, JYZ,
433 RRZ, XPW, and XZZ collected and analysed data over time, providing statistics and
434 material (graphs and tables) for the paper.

435

436 **Competing interests.** The authors declare that they have no conflict of interest.

437 **Acknowledgements.** This research received financial support from the National

438 Natural Science Foundation of China (41601562), the Strategic Priority Research
439 Program of the Chinese Academy of Sciences (XDA13020506) and China
440 Scholarship Council. The authors sincerely thank James Howard Stagge for his help
441 on the codes and calculation of SPEI. Special thanks go to the meteorological data
442 provider from China Meteorological Administration (<http://cdc.cma.gov.cn/>).

443

444 **References:**

- 445 Agrawala, S., Barlow, M., Cullen, H., and Lyon, B.: The drought and humanitarian crisis in Central and
446 Southwest Asia: a climate perspective, IRI special report N. 01-11, International Research Institute for
447 Climate Prediction, Palisades, 24, 2001.
- 448 Barella-Ortiz, A. and Quintana-Seguí, P.: Evaluation of drought representation and propagation in
449 regional climate model simulations across Spain, *Hydrology and Earth System Sciences*, 23, 5111-5131,
450 2019.
- 451 Boroneant, C., Ionita, M., Brunet, M., and Rimbu, N.: CLIVAR-SPAIN contributions: seasonal drought
452 variability over the Iberian Peninsula and its relationship to global sea surface temperature and large
453 scale atmospheric circulation, *WCRP OSC: Climate Research in Service to Society*, 2011. 24-28, 2011.
- 454 Bussi, G. and Whitehead, P. G.: Impacts of droughts on low flows and water quality near power
455 stations, *Hydrological Sciences Journal*, 65, 898-913, 2020.
- 456 Carlson, T. N., Gillies, R. R., and Perry, E. M.: A method to make use of thermal infrared temperature
457 and NDVI measurements to infer surface soil water content and fractional vegetation cover, *Remote
458 sensing reviews*, 9, 161-173, 1994.
- 459 Chen, C., Wang, E., and Yu, Q.: Modelling the effects of climate variability and water management on
460 crop water productivity and water balance in the North China Plain, *Agricultural Water Management*,
461 97, 1175-1184, 2010.
- 462 Dai, A., Trenberth, K. E., and Qian, T.: A global dataset of Palmer Drought Severity Index for 1870–2002:
463 Relationship with soil moisture and effects of surface warming, *Journal of Hydrometeorology*, 5,
464 1117-1130, 2004.
- 465 Doesken, N. and Garen, D.: Drought monitoring in the Western United States using a surface water
466 supply index, 1991, 10-13.
- 467 Eslamian, S., Ostad-Ali-Askari, K., Singh, V. P., Dalezios, N. R., Ghane, M., Yihdego, Y., and Matouq, M.:
468 A review of drought indices, *Int J Constr Res Civ Eng (IJRCRE)*, 3, 48-66, 2017.
- 469 Feng, K. and Su, X.: Spatiotemporal Characteristics of Drought in the Heihe River Basin Based on the
470 Extreme-Point Symmetric Mode Decomposition Method, *International Journal of Disaster Risk Science*,
471 10, 591-603, 2019.
- 472 Fuchs, B., Svoboda, M., Nothwehr, J., Poulsen, C., Sorensen, W., and Guttman, N.: A new national
473 drought risk Atlas for the US from the National Drought Mitigation Center, National Drought
474 Mitigation Center, Univ. of Nebraska: Lincoln, NE, USA, 2012. 2012.

475 Garrick, D. E., Hall, J. W., Dobson, A., Damania, R., Grafton, R. Q., Hope, R., Hepburn, C., Bark, R., Boltz,
476 F., and De Stefano, L.: Valuing water for sustainable development, *Science*, 358, 1003-1005, 2017.

477 Gevaert, A., Veldkamp, T., and Ward, P.: The effect of climate type on timescales of drought
478 propagation in an ensemble of global hydrological models, *Hydrology and Earth System Sciences*, 22,
479 4649-4665, 2018.

480 Grismer, M., Orang, M., Snyder, R., and Matyac, R.: Pan evaporation to reference evapotranspiration
481 conversion methods, *Journal of irrigation and drainage engineering*, 128, 180-184, 2002.

482 Han, X., Wu, J., Zhou, H., Liu, L., Yang, J., Shen, Q., and Wu, J.: Intensification of historical drought over
483 China based on a multi - model drought index, *International Journal of Climatology*, 2020. 2020.

484 Hargreaves, G. H. and Samani, Z. A.: Estimating potential evapotranspiration, *Journal of the Irrigation
485 and Drainage Division*, 108, 225-230, 1982.

486 Homdee, T., Pongput, K., and Kanae, S.: A comparative performance analysis of three standardized
487 climatic drought indices in the Chi River basin, Thailand, *Agriculture and Natural Resources*, 50,
488 211-219, 2016.

489 Jevšenak, J.: Daily climate data reveal stronger climate-growth relationships for an extended European
490 tree-ring network, *Quaternary Science Reviews*, 221, 105868, 2019.

491 Jia, Y., Zhang, B., and Ma, B.: Daily SPEI reveals long-term change in drought characteristics in
492 Southwest China, *Chinese Geographical Science*, 28, 680-693, 2018.

493 Kassaye, A. Y., Shao, G., Wang, X., and Wu, S.: Quantification of drought severity change in Ethiopia
494 during 1952–2017, *Environment, Development and Sustainability*, 2020. 1-26, 2020.

495 Kendall, M. G.: Rank correlation methods, 1948. 1948.

496 Kogan, F.: World droughts in the new millennium from AVHRR - based vegetation health indices, *Eos,
497 Transactions American Geophysical Union*, 83, 557-563, 2002.

498 Lai, C., Zhong, R., Wang, Z., Wu, X., Chen, X., Wang, P., and Lian, Y.: Monitoring hydrological drought
499 using long-term satellite-based precipitation data, *Science of the total environment*, 649, 1198-1208,
500 2019.

501 Li, Y., Yuan, X., Zhang, H., Wang, R., Wang, C., Meng, X., Zhang, Z., Wang, S., Yang, Y., and Han, B.:
502 Mechanisms and early warning of drought disasters: Experimental drought meteorology research over
503 China, *Bulletin of the American Meteorological Society*, 100, 673-687, 2019.

504 Lu, J., Sun, G., McNulty, S. G., and Amatya, D. M.: A Comparison of Six Potential Evapotranspiration
505 Methods for Regional Use in the Southeastern United States 1, *JAWRA Journal of the American Water
506 Resources Association*, 41, 621-633, 2005.

507 Makkink, G. F.: Testing the Penman formula by means of lysimeters, *Journal of the Institution of Water
508 Engineers*, 11, 277-288, 1957.

509 Mallya, G., Mishra, V., Niyogi, D., Tripathi, S., and Govindaraju, R. S.: Trends and variability of droughts
510 over the Indian monsoon region, *Weather and Climate Extremes*, 12, 43-68, 2016.

511 Mann, H.: Non-Parametric Tests against Trend. *Econometrica*, 13, 245-259, Mantua, NJ, SR Hare, Y.
512 Zhang, JM Wallace, and RC Francis (1997), *A Pacific decadal*, 1945. 1945.

513 Martí, P., Zarzo, M., Vanderlinden, K., and Girona, J.: Parametric expressions for the adjusted
514 Hargreaves coefficient in Eastern Spain, *Journal of Hydrology*, 529, 1713-1724, 2015.

515 McGUIRE, J. K. and Palmer, W. C.: The 1957 drought in the eastern United States, *Mon. Weather Rev*,
516 85, 305-314, 1957.

517 McKee, T. B., Doesken, N. J., and Kleist, J.: The relationship of drought frequency and duration to time
518 scales, 1993, 179-183.

519 Men-xin, W. and Hou-quan, L.: A modified vegetation water supply index (MVWSI) and its application
520 in drought monitoring over Sichuan and Chongqing, China, *Journal of Integrative Agriculture*, 15,
521 2132-2141, 2016.

522 Mendicino, G. and Senatore, A.: Regionalization of the Hargreaves coefficient for the assessment of
523 distributed reference evapotranspiration in Southern Italy, *Journal of Irrigation and Drainage*
524 *Engineering*, 139, 349-362, 2013.

525 Mishra, A. K. and Singh, V. P.: A review of drought concepts, *Journal of hydrology*, 391, 202-216, 2010.

526 Monish, N. and Rehana, S.: Suitability of distributions for standard precipitation and
527 evapotranspiration index over meteorologically homogeneous zones of India, *Journal of Earth System*
528 *Science*, 129, 25, 2020.

529 Morton, F. I.: Operational estimates of areal evapotranspiration and their significance to the science
530 and practice of hydrology, *Journal of Hydrology*, 66, 1-76, 1983.

531 Pendergrass, A. G., Meehl, G. A., Pulwarty, R., Hobbins, M., Hoell, A., AghaKouchak, A., Bonfils, C. J.,
532 Gallant, A. J., Hoerling, M., and Hoffmann, D.: Flash droughts present a new challenge for
533 subseasonal-to-seasonal prediction, *Nature Climate Change*, 10, 191-199, 2020.

534 Penman, H. L.: Natural evaporation from open water, bare soil and grass, *Proceedings of the Royal*
535 *Society of London. Series A. Mathematical and Physical Sciences*, 193, 120-145, 1948.

536 Potoč, V., Boroneanț, C., Možný, M., Štěpánek, P., and Skalák, P.: Observed spatiotemporal
537 characteristics of drought on various time scales over the Czech Republic, *Theoretical and applied*
538 *climatology*, 115, 563-581, 2014.

539 Priestley, C. H. B. and Taylor, R.: On the assessment of surface heat flux and evaporation using
540 large-scale parameters, *Monthly weather review*, 100, 81-92, 1972.

541 Salvador, C., Nieto, R., Linares, C., Diaz, J., and Gimeno, L.: Effects on daily mortality of droughts in
542 Galicia (NW Spain) from 1983 to 2013, *Science of The Total Environment*, 662, 121-133, 2019.

543 Sen, P. K.: Estimates of the regression coefficient based on Kendall's tau, *Journal of the American*
544 *statistical association*, 63, 1379-1389, 1968.

545 Sheffield, J., Andreadis, K., Wood, E. F., and Lettenmaier, D.: Global and continental drought in the
546 second half of the twentieth century: severity–area–duration analysis and temporal variability of
547 large-scale events, *Journal of Climate*, 22, 1962-1981, 2009.

548 Sohn, S. J., Ahn, J. B., and Tam, C. Y.: Six month–lead downscaling prediction of winter to spring
549 drought in South Korea based on a multimodel ensemble, *Geophysical Research Letters*, 40, 579-583,
550 2013.

551 Stagge, J. H., Tallaksen, L. M., Gudmundsson, L., Van Loon, A. F., and Stahl, K.: Candidate distributions
552 for climatological drought indices (SPI and SPEI), *International Journal of Climatology*, 35, 4027-4040,
553 2015.

554 Thomas, A.: Spatial and temporal characteristics of potential evapotranspiration trends over China,
555 *International Journal of Climatology: A Journal of the Royal Meteorological Society*, 20, 381-396, 2000.

556 Thornthwaite, C.: Report of the Committee on Transpiration and Evaporation 1943-44, *Transactions of*
557 *the American Geophysical Union*, 25, 683-693, 1944.

558 Tirivarombo, S., Osupile, D., and Eliasson, P.: Drought monitoring and analysis: standardised
559 precipitation evapotranspiration index (SPEI) and standardised precipitation index (SPI), *Physics and*
560 *Chemistry of the Earth, Parts A/B/C*, 106, 1-10, 2018.

561 Trenberth, K. E., Dai, A., Van Der Schrier, G., Jones, P. D., Barichivich, J., Briffa, K. R., and Sheffield, J.:
562 Global warming and changes in drought, *Nature Climate Change*, 4, 17-22, 2014.

563 Van der Schrier, G., Jones, P., and Briffa, K.: The sensitivity of the PDSI to the Thornthwaite and
564 Penman - Monteith parameterizations for potential evapotranspiration, *Journal of Geophysical*
565 *Research: Atmospheres*, 116, 2011.

566 Vicente-Serrano, S. M., Beguería, S., and López-Moreno, J. I.: A multiscalar drought index sensitive to
567 global warming: the standardized precipitation evapotranspiration index, *Journal of climate*, 23,
568 1696-1718, 2010.

569 Vicente-Serrano, S. M., López-Moreno, J. I., Beguería, S., Lorenzo-Lacruz, J., Azorin-Molina, C., and
570 Morán-Tejeda, E.: Accurate computation of a streamflow drought index, *Journal of Hydrologic*
571 *Engineering*, 17, 318-332, 2012.

572 Wan, Z., Wang, P., and Li, X.: Using MODIS land surface temperature and normalized difference
573 vegetation index products for monitoring drought in the southern Great Plains, USA, *International*
574 *journal of remote sensing*, 25, 61-72, 2004.

575 Wang, Q.-f., Tang, J., Zeng, J.-y., Qu, Y.-p., Zhang, Q., Shui, W., WANG, W.-l., Yi, L., and Leng, S.:
576 Spatial-temporal evolution of vegetation evapotranspiration in Hebei Province, China, *Journal of*
577 *Integrative Agriculture*, 17, 2107-2117, 2018.

578 Wang, Q., Qi, J., Li, J., Cole, J., Waldhoff, S. T., and Zhang, X.: Nitrate loading projection is sensitive to
579 freeze-thaw cycle representation, *Water Research*, 186, 116355, 2020a.

580 Wang, Q., Qi, J., Wu, H., Zeng, Y., Shui, W., Zeng, J., and Zhang, X.: Freeze-Thaw cycle representation
581 alters response of watershed hydrology to future climate change, *Catena*, 195, 104767, 2020b.

582 Wang, Q., Shi, P., Lei, T., Geng, G., Liu, J., Mo, X., Li, X., Zhou, H., and Wu, J.: The alleviating trend of
583 drought in the Huang - Huai - Hai Plain of China based on the daily SPEI, *International Journal of*
584 *Climatology*, 35, 3760-3769, 2015.

585 Wang, Q., Wu, J., Lei, T., He, B., Wu, Z., Liu, M., Mo, X., Geng, G., Li, X., and Zhou, H.: Temporal-spatial
586 characteristics of severe drought events and their impact on agriculture on a global scale, *Quaternary*
587 *International*, 349, 10-21, 2014.

588 Wang, Q., Zeng J., Qi J., Zhang, X., Zeng, Y., Shui, W., Xu. Z., Zhang, R., Wu, X.: 2020c: muliti-scale
589 daily SPEI dataset over the Mainland China from 1961-2018 (version June 2020),
590 available at figshare, <https://doi.org/10.6084/m9.figshare.12568280>

591 Wang, Q., Wu, J., Li, X., Zhou, H., Yang, J., Geng, G., An, X., Liu, L., and Tang, Z.: A comprehensively
592 quantitative method of evaluating the impact of drought on crop yield using daily multi-scale SPEI and
593 crop growth process model, *International journal of biometeorology*, 61, 685-699, 2017.

594 Wang, Y., Zhao, W., Zhang, Q., and Yao, Y.-b.: Characteristics of drought vulnerability for maize in the
595 eastern part of Northwest China, *Scientific reports*, 9, 1-9, 2019.

596 Wilhite, D. A. and Glantz, M. H.: Understanding: the drought phenomenon: the role of definitions,
597 *Water international*, 10, 111-120, 1985.

598 Yang, P., Xia, J., Zhang, Y., Zhan, C., and Qiao, Y.: Comprehensive assessment of drought risk in the arid
599 region of Northwest China based on the global palmer drought severity index gridded data, *Science of*
600 *the Total Environment*, 627, 951-962, 2018.

601 Yevjevich, V. M.: Objective approach to definitions and investigations of continental hydrologic
602 droughts, *An, Hydrology papers (Colorado State University)*; no. 23, 1967. 1967.

603 Yu, M., Li, Q., Hayes, M. J., Svoboda, M. D., and Heim, R. R.: Are droughts becoming more frequent or
604 severe in China based on the standardized precipitation evapotranspiration index: 1951–2010?,
605 *International Journal of Climatology*, 34, 545-558, 2014.

606 Zambrano, F., Vrieling, A., Nelson, A., Meroni, M., and Tadesse, T.: Prediction of drought-induced

607 reduction of agricultural productivity in Chile from MODIS, rainfall estimates, and climate oscillation
608 indices, Remote sensing of environment, 219, 15-30, 2018.

609 Zargar, A., Sadiq, R., Naser, B., and Khan, F. I.: A review of drought indices, Environmental Reviews, 19,
610 333-349, 2011.

611